

4. The Riemann Problem for the Euler Equations

In his classical paper of 1959, Godunov [130] presented a conservative extension of the first-order upwind scheme of Courant, Isaacson and Rees [89] to non-linear systems of hyperbolic conservation laws. The key ingredient of the scheme is the solution of the Riemann problem. The purpose of this chapter is to provide a detailed presentation of the complete, exact solution to the Riemann problem for the one-dimensional, time-dependent Euler equations for ideal and covolume gases, including vacuum conditions. The methodology can then be applied to other hyperbolic systems.

The exact solution to the Riemann problem is useful in a number of ways. First, it represents the solution to a system of hyperbolic conservation laws subject to the simplest, non-trivial, initial conditions; it nevertheless contains the fundamental physical and mathematical character of the relevant set of conservation laws. The solution of the general IVP may be seen as resulting from non-linear superposition of solutions of local Riemann problems [127]. In the case of the Euler equations the Riemann problem contains the so called *shock-tube problem*, a basic physical problem in Gas Dynamics. For a detailed discussion on the shock-tube problem the reader is referred to the book by Courant and Friedrichs [88]. The exact Riemann problem solution is also an invaluable reference solution that is useful in assessing the performance of numerical methods and to check the correctness of programs in the early stages of development. The Riemann problem solution, exact or approximate, can also be used locally in the method of Godunov and high-order extensions of it; this is the main role we assign to the Riemann problem here. A detailed knowledge of the exact solution is also fundamental when utilising, assessing and developing approximate Riemann solvers.

There is no exact closed-form solution to the Riemann problem for the Euler equations, not even for ideal gases; in fact not even for much simpler models such as the isentropic and isothermal equations. However, it is possible to devise *iterative* schemes whereby the solution can be computed numerically to any desired, practical, degree of accuracy. Key issues in designing an exact Riemann solver are: the variables selected, the equations used, the number of equations and the technique for the iterative procedure, the initial guess and the handling of unphysical iterates, such as negative pressure. Godunov is credited with the first exact Riemann solver for the Euler equations [130].

By today's standards Godunov's first Riemann solver is cumbersome and computationally inefficient. Later, Godunov [132] proposed a second exact Riemann solver. Distinct features of this solver are: the equations used are simpler, the variables selected are more convenient from the computational point of view and the iterative procedure is rather sophisticated. Much of the work that followed contains the fundamental features of Godunov's second Riemann solver. Chorin [65], independently, produced improvements to Godunov's first Riemann solver. In 1979, van Leer [356] produced another improvement to Godunov's first Riemann solver resulting in a scheme that is similar to Godunov's second solver. Smoller [289] proposed a rather different approach; later, Dutt [103] produced a practical implementation of the scheme. Gottlieb and Groth [135] presented another Riemann solver for ideal gases; of the schemes they tested, theirs is shown to be the most efficient. Toro [323] presented an exact Riemann solver for ideal and covolume gases of comparable efficiency to that of Gottlieb and Groth. More recently, Schleicher [273] and Pike [238] have also presented new exact Riemann solvers which appear to be the fastest to date. For gases obeying a general equation of state the reader is referred to the pioneering work of Colella and Glaz [81]. Other relevant publications are that of Menikoff and Plohr [217] and that of Saurel, Larini and Loraud [272].

In this chapter we present a solution procedure of the Riemann problem for the Euler equations for both ideal and covolume gases. The methodology is presented in great detail for the ideal gas case. We then address the issue of *vacuum* and provide an exact solution for the three cases that can occur. Particular emphasis is given to the *sampling* of the solution; this will be useful to provide the complete solution and to utilise it in numerical methods such as the Godunov method [130] and Glimm's method or Random Choice Method [127], [65]. The necessary background for this chapter is found in Chaps. 1, 2 and 3.

4.1 Solution Strategy

The Riemann problem for the one-dimensional time-dependent Euler equations is the Initial Value Problem (IVP) for the conservation laws

$$\begin{aligned} \mathbf{U}_t + \mathbf{F}(\mathbf{U})_x &= \mathbf{0}, \\ \mathbf{U} = \left[\begin{array}{c} \rho \\ \rho u \\ E \end{array} \right], \quad \mathbf{F} = \left[\begin{array}{c} \rho u \\ \rho u^2 + p \\ u(E + p) \end{array} \right], \end{aligned} \quad \left. \right\} \quad (4.1)$$

with initial conditions (IC)

$$\mathbf{U}(x, 0) = \mathbf{U}^{(0)}(x) = \begin{cases} \mathbf{U}_L & \text{if } x < 0, \\ \mathbf{U}_R & \text{if } x > 0. \end{cases} \quad (4.2)$$

The domain of interest in the $x-t$ plane are points (x, t) with $-\infty < x < \infty$ and $t > 0$. In practice one lets x vary in a finite interval $[x_L, x_R]$ around the point $x = 0$. In solving the Riemann problem we shall frequently make use of the vector $\mathbf{W} = (\rho, u, p)^T$ of primitive variables, rather than the vector \mathbf{U} of conserved variables, where ρ is density, u is particle velocity and p is pressure. The Riemann problem (4.1)–(4.2) is the simplest, non-trivial, IVP for (4.1). Data consists of just two constant states, which in terms of primitive variables are $\mathbf{W}_L = (\rho_L, u_L, p_L)^T$ to the left of $x = 0$ and $\mathbf{W}_R = (\rho_R, u_R, p_R)^T$ to the right of $x = 0$, separated by a discontinuity at $x = 0$. Physically, in the context of the Euler equations, the Riemann problem is a slight generalisation of the so called *shock-tube problem*: two stationary gases ($u_L = u_R = 0$) in a tube are separated by a diaphragm. The rupture of the diaphragm generates a nearly centred wave system that typically consists of a rarefaction wave, a contact discontinuity and a shock wave. This physical problem is reasonably well approximated by solving the shock-tube problem for the Euler equations. In the Riemann problem the particle speeds u_L and u_R are allowed to be non-zero, but the structure of the solution is the same as that of the shock-tube problem. In general, given the conservation equations (4.1) for

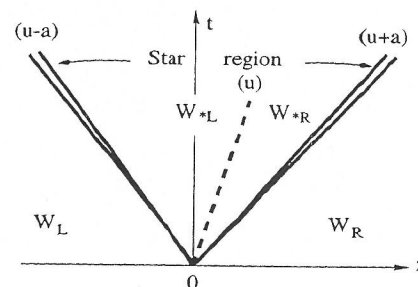


Fig. 4.1. Structure of the solution of the Riemann problem on the x - t plane for the one-dimensional time-dependent Euler equations

the dynamics, it is left to the statements about the material, the equation of state, to determine not only the structure of the solution of the Riemann problem but also the mathematical character of the equations. In this chapter we restrict our attention to *ideal gases* obeying the caloric Equation of State (EOS)

$$e = \frac{p}{(\gamma - 1)\rho}, \quad (4.3)$$

and *covolume gases* obeying

$$e = \frac{p(1 - b\rho)}{(\gamma - 1)\rho}, \quad (4.4)$$

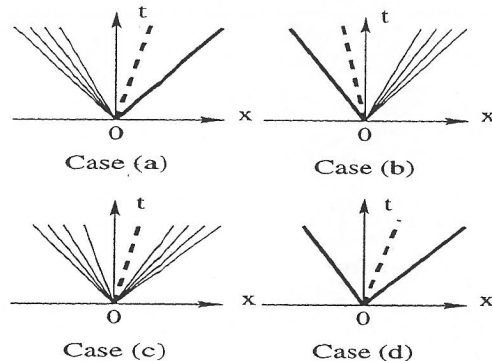


Fig. 4.2. Possible wave patterns in the solution of the Riemann problem: (a) left rarefaction, contact, right shock (b) left shock, contact, right rarefaction (c) left rarefaction, contact, right rarefaction (d) left shock, contact, right shock

where γ is the ratio of specific heats, a constant, and b is the covolume, also a constant. See Sects. 1.2.4 and 1.2.5 of Chap. 1. For the case in which no *vacuum* is present the exact solution of the Riemann problem (4.1), (4.2) has three waves, which are *associated* with the eigenvalues $\lambda_1 = u - a$, $\lambda_2 = u$ and $\lambda_3 = u + a$; see Fig. 4.1. Note that the speeds of these waves are not, in general, the characteristic speeds given by the eigenvalues. The three waves separate four constant states, which from left to right are: W_L (data on the left hand side), W_{*L} , W_{*R} and W_R (data on the right hand side).

The unknown region between the left and right waves, the *Star Region*, is divided by the middle wave into the two subregions *Star Left* (W_{*L}) and *Star Right* (W_{*R}). As seen in Sect. 3.1.3 of Chap. 3, the middle wave is always a contact discontinuity while the left and right (non-linear) waves are either shock or rarefaction waves. Therefore, according to the type of non-linear waves there can be four possible wave patterns, which are shown in Fig. 4.2. There are two variations of these which are only of interest when utilising the solution in Godunov-type methods, namely when a non-linear wave is a *sonic rarefaction wave*. For the purpose of constructing a solution scheme for the Riemann problem it is sufficient to consider the four patterns of Fig. 4.2.

An analysis based on the eigenstructure of the Euler equations, Sect. 3.1.3 Chap. 3, reveals that both pressure p_* and particle velocity u_* between the left and right waves are constant, while the density takes on the two constant values ρ_{*L} and ρ_{*R} . Here we present a solution procedure which makes use of the constancy of pressure and particle velocity in the *Star Region* to derive a single, algebraic non-linear equation for pressure p_* . In summary, the main physical quantities sought are p_* , u_* , ρ_{*L} and ρ_{*R} .

4.2 Equations for Pressure and Particle Velocity

Here we establish equations and solution strategies for computing the pressure p_* and the particle velocity u_* in the *Star Region*.

Proposition 4.2.1 (solution for p_* and u_*). *The solution for pressure p_* of the Riemann problem (4.1), (4.2) with the ideal gas Equation of State (4.3) is given by the root of the algebraic equation*

$$f(p, W_L, W_R) \equiv f_L(p, W_L) + f_R(p, W_R) + \Delta u = 0, \quad \Delta u \equiv u_R - u_L, \quad (4.5)$$

where the function f_L is given by

$$f_L(p, W_L) = \begin{cases} (p - p_L) \left[\frac{A_L}{p + B_L} \right]^{\frac{1}{2}} & \text{if } p > p_L \text{ (shock)}, \\ \frac{2a_L}{(\gamma-1)} \left[\left(\frac{p}{p_L} \right)^{\frac{\gamma-1}{2\gamma}} - 1 \right] & \text{if } p \leq p_L \text{ (rarefaction)}, \end{cases} \quad (4.6)$$

the function f_R is given by

$$f_R(p, W_R) = \begin{cases} (p - p_R) \left[\frac{A_R}{p + B_R} \right]^{\frac{1}{2}} & \text{if } p > p_R \text{ (shock)}, \\ \frac{2a_R}{(\gamma-1)} \left[\left(\frac{p}{p_R} \right)^{\frac{\gamma-1}{2\gamma}} - 1 \right] & \text{if } p \leq p_R \text{ (rarefaction)}, \end{cases} \quad (4.7)$$

and the data-dependent constants A_L , B_L , A_R , B_R are given by

$$\left. \begin{aligned} A_L &= \frac{2}{(\gamma+1)p_L}, & B_L &= \frac{(\gamma-1)}{(\gamma+1)}p_L, \\ A_R &= \frac{2}{(\gamma+1)p_R}, & B_R &= \frac{(\gamma-1)}{(\gamma+1)}p_R. \end{aligned} \right\} \quad (4.8)$$

The solution for the particle velocity u_* in the *Star Region* is

$$u_* = \frac{1}{2}(u_L + u_R) + \frac{1}{2}[f_R(p_*) - f_L(p_*)]. \quad (4.9)$$

Remark 4.2.1. Before proceeding to prove the above statements we make some useful remarks. Once (4.5) is solved for p_* the solution for u_* follows as in (4.9) and the remaining unknowns are found by using standard gas dynamics relations studied in Chap. 3. The function f_L governs relations across the left non-linear wave and serves to connect the unknown particle speed u_* to the known state W_L on the left side, see Fig. 4.3; the relations depend on the type of wave (shock or rarefaction). The arguments of f_L are the pressure p and the data state W_L . Similarly, the function f_R governs relations across the right wave and connects the unknown u_* to the right data state W_R ; its arguments are p and W_R . For convenience we shall often omit the data arguments of the functions f , f_L and f_R . The sought pressure

p_* in the *Star Region* is the root of the algebraic equation (4.5), $f(p) = 0$. A detailed analysis of the pressure function $f(p)$ reveals a particularly simple behaviour and that for *physically relevant data* there exists a unique solution to the equation $f(p) = 0$.

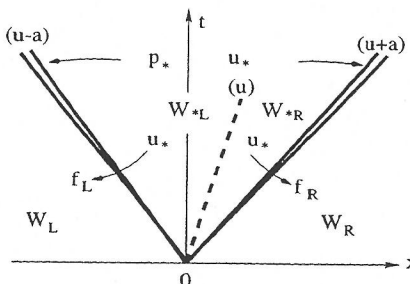


Fig. 4.3. Strategy for solving the Riemann problem via a pressure function. The particle velocity is connected to data on the left and right via functions f_L and f_R

Proof. Here we derive expressions for f_L and f_R in equation (4.5). We do this by considering each non-linear wave separately.

(4.5) will be proved using $\Delta u \equiv u_R - u_L = (u_R - u_x) + (u_x - u_L)$ and finding appropriate expressions for $u_R - u_x$, $u_x - u_L$.

4.2.1 Function f_L for a Left Shock

We assume the left wave is a shock moving with speed S_L as shown in Fig. 4.4a; pre-shock values are ρ_L , u_L and p_L and post-shock values are ρ_{*L} , u_* and p_* .

As done in Sect. 3.1.3 of Chap. 3, we transform the equations to a frame of reference moving with the shock, as depicted in Fig. 4.4b. In the new frame the shock speed is zero and the *relative velocities* are

$$\hat{u}_L = u_L - S_L, \quad \hat{u}_* = u_* - S_L. \quad (4.10)$$

The Rankine–Hugoniot Conditions, see Sect. 3.1.3 of Chap. 3, give

$$\rho_L \hat{u}_L = \rho_{*L} \hat{u}_*, \quad (4.11)$$

$$\rho_L \hat{u}_L^2 + p_L = \rho_{*L} \hat{u}_*^2 + p_*, \quad (4.12)$$

$$\hat{u}_L (\hat{E}_L + p_L) = \hat{u}_* (\hat{E}_{*L} + p_*). \quad (4.13)$$

We introduce the *mass flux* Q_L , which in view of (4.11) may be written as

$$Q_L \equiv \rho_L \hat{u}_L = \rho_{*L} \hat{u}_*. \quad (4.14)$$

From equation (4.12)

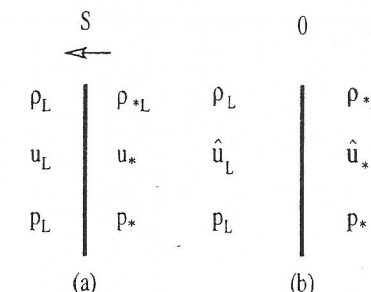


Fig. 4.4. Left wave is a shock wave of speed S_L : (a) stationary frame, shock speed is S_L (b) frame of reference moving with speed S_L , shock speed is zero

$$(\rho_L \hat{u}_L) \hat{u}_L + p_L = (\rho_{*L} \hat{u}_*) \hat{u}_* + p_*. \quad (4.15)$$

Use of (4.14) and solving for Q_L gives

$$Q_L = -\frac{p_* - p_L}{\hat{u}_* - \hat{u}_L}. \quad (4.15)$$

But from equation (4.10) $\hat{u}_L - \hat{u}_* = u_L - u_*$ and so Q_L becomes

$$Q_L = -\frac{p_* - p_L}{u_* - u_L}, \quad (4.16)$$

from which we obtain

$$u_* = u_L - \frac{(p_* - p_L)}{Q_L}. \quad (4.17)$$

We are now close to having related u_* to data on the left hand side. We seek to express the right hand side of (4.17) purely in terms of p_* and W_L , which means that we need to express Q_L as a function of p_* and the data on the left hand side. We substitute the relations

$$\hat{u}_L = \frac{Q_L}{\rho_L}, \quad \hat{u}_* = \frac{Q_L}{\rho_{*L}},$$

obtained from (4.14) into equation (4.15) to produce

$$Q_L^2 = -\frac{p_* - p_L}{\frac{1}{\rho_{*L}} - \frac{1}{\rho_L}}. \quad (4.18)$$

As seen in Sect. 3.1.3 of Chap. 3, the density ρ_{*L} is related to the pressure p_* behind the left shock via

$$\rho_{*L} = \rho_L \left[\frac{\left(\frac{\gamma-1}{\gamma+1} \right) + \left(\frac{p_*}{p_L} \right)}{\left(\frac{\gamma-1}{\gamma+1} \right) \left(\frac{p_*}{p_L} \right) + 1} \right]. \quad (4.19)$$

Substitution of ρ_{*L} into (4.18) yields

$$Q_L = \left[\frac{p_* + B_L}{A_L} \right]^{\frac{1}{2}}, \quad (4.20)$$

which in turn reduces (4.17) to

$$u_* = u_L - f_L(p_*, W_L), \quad (4.21)$$

with

$$f_L(p_*, W_L) = (p_* - p_L) \left[\frac{A_L}{p_* + B_L} \right]^{\frac{1}{2}}$$

and

$$A_L = \frac{2}{(\gamma + 1)\rho_L}, \quad B_L = \frac{(\gamma - 1)}{(\gamma + 1)}p_L.$$

Thus, the sought expression for f_L for the case in which the left wave is a shock wave has been obtained.

4.2.2 Function f_L for Left Rarefaction

Now we derive an expression for f_L for the case in which the left wave is a rarefaction wave, as shown in Fig. 4.5. The unknown state W_{*L} is now connected to the left data state W_L using the isentropic relation and the Generalised Riemann Invariants for the left wave. As seen in Sect. 3.1.2 of

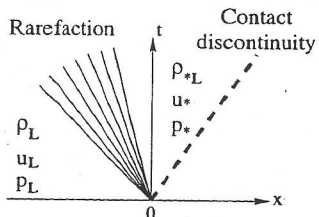


Fig. 4.5. Left wave is a rarefaction wave that connects the data state W_L with the unknown state W_{*L} in the star region to the left of the contact discontinuity

Chap. 3, the isentropic law

$$p = C\rho^\gamma, \quad (4.22)$$

where C is a constant, may be used across rarefactions. C is evaluated at the *initial* left data state by applying the isentropic law, namely

$$p_L = C\rho_L^\gamma,$$

and so the constant C is

$$C = p_L/\rho_L^\gamma,$$

from which we write

$$\rho_{*L} = \rho_L \left(\frac{p_*}{p_L} \right)^{\frac{1}{\gamma}}. \quad (4.23)$$

In Sect. 3.1.3 of Chap. 3 we showed that across a left rarefaction the Generalised Riemann Invariant $I_L(u, a)$ is constant. By evaluating the constant on the left data state we write

$$u_L + \frac{2a_L}{\gamma - 1} = u_* + \frac{2a_{*L}}{\gamma - 1}, \quad (4.24)$$

where a_L and a_{*L} denote the sound speed on the left and right states bounding the left rarefaction wave. See Fig. 4.5.

Substitution of ρ_{*L} from (4.23) into the definition of a_{*L} gives

$$a_{*L} = a_L \left(\frac{p_*}{p_L} \right)^{\frac{\gamma-1}{2\gamma}}, \quad (4.25)$$

and equation (4.24) leads to

$$u_* = u_L - f_L(p_*, W_L), \quad (4.26)$$

with

$$f_L(p_*, W_L) = \frac{2a_L}{(\gamma - 1)} \left[\left(\frac{p_*}{p_L} \right)^{\frac{\gamma-1}{2\gamma}} - 1 \right].$$

This is the required expression for the function f_L for the case in which the left wave is a rarefaction wave.

4.2.3 Function f_R for a Right Shock

Here we find the expression for the function f_R for the case in which the right wave is a shock wave travelling with speed S_R . The situation is entirely analogous to the case of a left shock wave. Pre-shock values are ρ_R , u_R and p_R and post-shock values are ρ_{*R} , u_* and p_* . In the transformed frame of reference moving with the shock, the shock speed is zero and the relative velocities are

$$\hat{u}_R = u_R - S_R, \quad \hat{u}_* = u_* - S_R. \quad (4.27)$$

Application of the Rankine–Hugoniot Conditions gives

$$\left. \begin{aligned} \rho_{*R}\hat{u}_* &= \rho_R\hat{u}_R, \\ \rho_{*R}\hat{u}_*^2 + p_* &= \rho_R\hat{u}_R^2 + p_R, \\ \hat{u}_*(\hat{E}_{*R} + p_*) &= \hat{u}_R(\hat{E}_R + p_R). \end{aligned} \right\} \quad (4.28)$$

Now the *mass flux* is defined as

$$Q_R \equiv -\rho_{*R}\hat{u}_* = -\rho_R\hat{u}_R. \quad (4.29)$$

By performing algebraic manipulations similar to those for a left shock we derive the following expression for the mass flux

$$Q_R = \left[\frac{p_* + B_R}{A_R} \right]^{\frac{1}{2}}. \quad (4.30)$$

Hence the particle velocity in the *Star Region* satisfies

$$u_* = u_R + f_R(p_*, W_R), \quad (4.31)$$

with

$$f_R(p_*, W_R) = (p_* - p_R) \left[\frac{A_R}{p_* + B_R} \right]^{\frac{1}{2}},$$

$$A_R = \frac{2}{(\gamma + 1)p_R}, \quad B_R = \frac{(\gamma - 1)}{(\gamma + 1)}p_R.$$

This is the sought expression for f_R for the case in which the right wave is a shock wave.

4.2.4 Function f_R for a Right Rarefaction

The derivation of the function f_R for the case in which the right wave is a rarefaction wave is carried out in an entirely analogous manner to the case of a left rarefaction. The isentropic law gives

$$\rho_{*R} = \rho_R \left(\frac{p_*}{p_R} \right)^{\frac{1}{\gamma}} \quad (4.32)$$

and the Generalised Riemann Invariant $I_R(u, a)$ for a right rarefaction gives

$$u_* - \frac{2a_{*R}}{\gamma - 1} = u_R - \frac{2a_R}{\gamma - 1}. \quad (4.33)$$

Using (4.32) into the definition of sound speed a_{*R} gives

$$a_{*R} = a_R \left(\frac{p_*}{p_R} \right)^{\frac{\gamma-1}{2\gamma}}, \quad (4.34)$$

which if substituted into (4.33) leads to

$$u_* = u_R + f_R(p_*, W_R), \quad (4.35)$$

with

$$f_R(p_*, W_R) = \frac{2a_R}{\gamma - 1} \left[\left(\frac{p_*}{p_R} \right)^{\frac{\gamma-1}{2\gamma}} - 1 \right].$$

The functions f_L and f_R have now been determined for all four possible wave patterns of Fig. 4.2. Now by eliminating u_* from equations (4.21) or (4.26) and (4.31) or (4.35) we obtain a single equation

$$f(p_*, W_L, W_R) \equiv f_L(p_*, W_L) + f_R(p_*, W_R) + \Delta u = 0, \quad (4.36)$$

which is the required equation (4.5) for the pressure. This proves the first part of the proposition. Assuming this single non-linear algebraic equation is solved (numerically) for p_* then the solution for the particle velocity u_* can be found from equation (4.21) if the left wave is a shock ($p_* > p_L$) or from equation (4.26) if the left wave is a rarefaction ($p_* \leq p_L$) or from equation (4.31) if the right wave is a shock ($p_* > p_R$) or from equation (4.35) if the right wave is a rarefaction wave ($p_* \leq p_R$). It can also be found from a mean value as

$$u_* = \frac{1}{2}(u_L + u_R) + \frac{1}{2}[f_R(p_*) - f_L(p_*)],$$

which is equation (4.9), and the proposition has thus been proved.

4.3 Numerical Solution for Pressure

The unknown pressure p_* in the *Star Region* is found by solving the single algebraic equation (4.5), $f(p) = 0$, numerically. Any standard technique can be used. See Maron and Lopez [205] for background on numerical methods for algebraic equations. The behaviour of the pressure function $f(p)$ plays a fundamental role in finding its roots numerically.

4.3.1 Behaviour of the Pressure Function

Given data ρ_L, u_L, p_L and ρ_R, u_R, p_R the pressure function $f(p)$ behaves as shown in Fig. 4.6. It is monotone and concave down as we shall demonstrate.

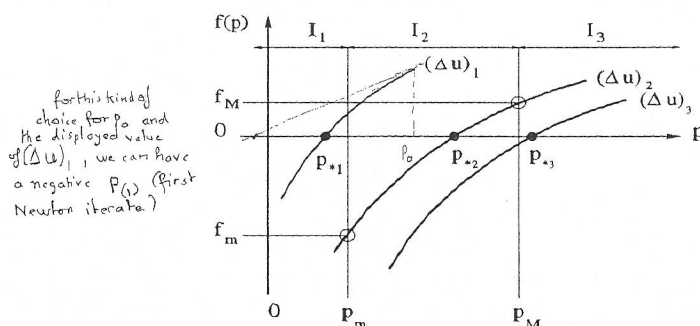


Fig. 4.6. Behaviour of the pressure function in the solution of the Riemann problem

The first derivatives of f_K ($K=L,R$) with respect to p are

$$f'_K = \begin{cases} \left(\frac{A_K}{B_K+p}\right)^{1/2} \left[1 - \frac{p-p_K}{2(B_K+p)}\right] & \text{if } p > p_K \text{ (shock)}, \\ \frac{1}{\rho_K a_K} \left(\frac{p}{p_K}\right)^{-(\gamma+1)/2\gamma} & \text{if } p \leq p_K \text{ (rarefaction)} . \end{cases} \quad (4.37)$$

As $f' = f'_L + f'_R$ and by inspection $f'_K > 0$, the function $f(p)$ is monotone as claimed. The second derivatives of the functions f_K are

$$f''_K = \begin{cases} -\frac{1}{4} \left(\frac{A_K}{B_K+p}\right)^{1/2} \left[\frac{4B_K+3p+p_K}{(B_K+p)^2}\right] & \text{if } p > p_K \text{ (shock)}, \\ -\frac{(\gamma+1)a_K}{2\gamma^2 p_K^2} \left(\frac{p}{p_K}\right)^{-(3\gamma+1)/2\gamma} & \text{if } p \leq p_K \text{ (rarefaction)} . \end{cases} \quad (4.38)$$

Since $f'' = f''_L + f''_R$ and $f''_K < 0$ the function $f(p)$ is concave down as anticipated. From equations (4.37) and (4.38) it can be seen that $f'_K \rightarrow 0$ as $p \rightarrow \infty$ and $f''_K \rightarrow 0$ as $p \rightarrow \infty$. This behaviour of f_K , and thus of $f(p)$, has implications when devising iteration schemes to find the zero p_* of $f(p) = 0$. The velocity difference $\Delta u = u_R - u_L$ and the pressure values p_L, p_R are the most important parameters of $f(p)$. With reference to Fig. 4.6 we define

$$p_{\min} = \min(p_L, p_R), \quad p_{\max} = \max(p_L, p_R),$$

$$f_{\min} = f(p_{\min}), \quad f_{\max} = f(p_{\max}).$$

For given p_L, p_R it is the velocity difference Δu which determines the value of p_* . Three intervals I_1, I_2 and I_3 can be identified:

$$\left. \begin{array}{ll} p_* \text{ lies in } I_1 = (0, p_{\min}) & \text{if } f_{\min} > 0 \text{ and } f_{\max} > 0, \\ p_* \text{ lies in } I_2 = [p_{\min}, p_{\max}] & \text{if } f_{\min} \leq 0 \text{ and } f_{\max} \geq 0, \\ p_* \text{ lies in } I_3 = (p_{\max}, \infty) & \text{if } f_{\min} < 0 \text{ and } f_{\max} < 0. \end{array} \right\} \quad (4.39)$$

For sufficiently large Δu , as $(\Delta u)_1$ in Fig. 4.6, the solution p_* is as p_{*1} , which lies in I_1 and thus $p_* < p_L, p_* < p_R$; so the two non-linear waves are rarefaction waves. For Δu as $(\Delta u)_2$ in Fig. 4.6 $p_* = p_{*2}$ lies between p_L and p_R and hence one non-linear wave is a rarefaction wave and the other is a shock wave. For sufficiently small values of Δu , as $(\Delta u)_3$ in Fig. 4.6, $p_* = p_{*3}$ lies in I_3 , that is $p_* > p_L, p_* > p_R$, which means that both non-linear waves are shock waves. The interval where p_* lies is identified by noting the signs of f_{\min} and f_{\max} ; see 4.39.

Another observation on the behaviour of $f(p)$ is this: in I_1 both $f'(p)$ and $f''(p)$ vary rapidly; this may lead to numerical difficulties when searching for the root of $f(p) = 0$. As p increases the shape of $f(p)$ tends to resemble that of a straight line. For non-vacuum initial data $\mathbf{W}_L, \mathbf{W}_R$ there exists a unique positive solution p_* for pressure, provided Δu is sufficiently small. As

a matter of fact, even for the case in which the data states are *non-vacuum states*, values of Δu larger than a critical value $(\Delta u)_{\text{crit}}$ lead to vacuum in the solution of the Riemann problem. The critical value can be found analytically in terms of the initial data. Clearly for a positive solution for pressure p_* we require $f(0) < 0$. Direct evaluation of $f(p)$ gives the *pressure positivity condition*

$$(\Delta u)_{\text{crit}} \equiv \frac{2a_L}{\gamma-1} + \frac{2a_R}{\gamma-1} > u_R - u_L. \quad (4.40)$$

Vacuum is created by the non-linear waves if this condition is violated. The structure of the solution in this case is different from that depicted in Fig. 4.1 and so is the method of solution, as we shall see in Sect. 4.6 of this chapter.

4.3.2 Iterative Scheme for Finding the Pressure

Given the particularly simple behaviour of the pressure function $f(p)$ and the availability of analytic expressions for the derivative of $f(p)$ we use a Newton-Raphson [205] iterative procedure to find the root of $f(p) = 0$. Suppose a guess value p_0 for the true solution p_* is available; since $f(p)$ is a smooth function we can find an approximate value of $f(p)$ at a neighbouring point $p_0 + \delta$ via a Taylor expansion

$$f(p_0 + \delta) = f(p_0) + \delta f'(p_0) + O(\delta^2). \quad (4.41)$$

If the $p_0 + \delta$ is a solution of $f(p) = 0$ then

$$f(p_0) + \delta f'(p_0) = 0, \quad (4.42)$$

and so the *corrected* value $p_1 = p_0 + \delta$ is

$$p_1 = p_0 - \frac{f(p_0)}{f'(p_0)}. \quad (4.43)$$

The above procedure generalises to

$$p_{(k)} = p_{(k-1)} - \frac{f(p_{(k-1)})}{f'(p_{(k-1)})}, \quad (4.44)$$

where $p_{(k)}$ is the k -th iterate. The iteration procedure is stopped whenever the relative pressure change

$$CHA = \frac{|p_{(k)} - p_{(k-1)}|}{\frac{1}{2}[p_{(k)} + p_{(k-1)}]}, \quad (4.45)$$

is less than a prescribed small tolerance TOL . Typically $TOL = 10^{-6}$.

In order to implement the iteration scheme (4.44) we need a guess value p_0 for the pressure. Given the benign behaviour of $f(p)$ the choice of p_0 is not too critical. An inadequate choice of p_0 results in a large number of iterations to achieve convergence. A difficulty that requires special handling

in the Newton–Raphson method arises when the root is close to zero (strong rarefaction waves) and the guess value p_0 is too large: the next iterate for pressure can be negative. This is due to the rapid variations of the first and second derivatives of $f(p)$ near $p = 0$. We illustrate the effect of the initial guess value by considering four possible choices. Three of these are approximations to the solution p_* for pressure, see Chap. 9 for details. One such approximation is the so called *Two-Rarefaction* approximation

$$p_{\text{TR}} = \left[\frac{a_L + a_R - \frac{1}{2}(\gamma - 1)(u_R - u_L)}{a_L/p_L^{\frac{\gamma-1}{2\gamma}} + a_R/p_R^{\frac{\gamma-1}{2\gamma}}} \right]^{\frac{2\gamma}{\gamma-1}}, \quad (4.46)$$

and results from the exact function (4.5) for pressure under the assumption that the two non-linear waves are rarefaction waves. If the solution actually consists of two rarefactions then p_{TR} is exact and no iteration is required. A second guess value results from a linearised solution based on primitive variables. This is

$$\left. \begin{aligned} p_0 &= \max(TOL, p_{\text{PV}}), \\ p_{\text{PV}} &= \frac{1}{2}(p_L + p_R) - \frac{1}{8}(u_R - u_L)(\rho_L + \rho_R)(a_L + a_R). \end{aligned} \right\} \quad (4.47)$$

A third guess value is given by a *Two-Shock* approximation

$$\left. \begin{aligned} p_0 &= \max(TOL, p_{\text{TS}}), \\ p_{\text{TS}} &= \frac{g_L(\hat{p})p_L + g_R(\hat{p})p_R - \Delta u}{g_L(\hat{p}) + g_R(\hat{p})}, \\ g_K(p) &= \left(\frac{A_K}{p + B_K} \right)^{\frac{1}{2}}, \end{aligned} \right\} \quad (4.48)$$

where A_K and B_K given by (4.8). Here \hat{p} is an estimate of the solution; the value $\hat{p} = p_0$ given by (4.47) works well. Note that approximate solutions may predict, incorrectly, a negative value for pressure, even when condition (4.40) is satisfied. Thus in order to avoid negative guess values we introduce the small positive constant TOL , as used in the iteration procedure. As a fourth guess value we utilise the arithmetic mean of the data, namely

$$p_0 = \frac{1}{2}(p_L + p_R). \quad (4.49)$$

Next, we carry out some tests on the effect of the various guess values for p_0 on the convergence of the Newton–Raphson iterative scheme for finding the pressure p_* .

4.3.3 Numerical Tests

Five Riemann problems are selected to test the performance of the Riemann solver and the influence of the initial guess for pressure. The tests are also used to illustrate some typical wave patterns resulting from the solution of the Riemann problem. Table 4.1 shows the data for all five tests in terms of primitive variables. In all cases the ratio of specific heats is $\gamma = 1.4$.

Test 1 is the so called Sod test problem [291]; this is a very mild test and its solution consists of a left rarefaction, a contact and a right shock. Fig. 4.7 shows solution profiles for density, velocity, pressure and specific internal energy across the complete wave structure, at time $t = 0.25$ units. Test 2, called the *123 problem*, has solution consisting of two strong rarefactions and a trivial-stationary contact discontinuity; the pressure p_* is very small (close to vacuum) and this can lead to difficulties in the iteration scheme to find p_* numerically. Fig. 4.8 shows solution profiles. Test 2 is also useful in assessing the performance of numerical methods for low density flows, see Einfeldt et. al. [106]. Test 3 is a very severe test problem the solution of which contains a left rarefaction, a contact and a right shock; this test is actually the left half of the blast wave problem of Woodward and Colella [374] for which Fig. 4.9 shows solution profiles. Test 4 is the right half of the Woodward and Colella problem; its solution contains a left shock, a contact discontinuity and a right rarefaction, as shown in Fig. 4.10. Test 5 is made up of the right and left shocks emerging from the solution to tests 3 and 4 respectively; its solution represents the collision of these two strong shocks and consists of a left facing shock (travelling very slowly to the right), a right travelling contact discontinuity and a right travelling shock wave. Fig. 4.11 shows solution profiles for Test 5.

Test	ρ_L	u_L	p_L	ρ_R	u_R	p_R
1	1.0	0.0	1.0	0.125	0.0	0.1
2	1.0	-2.0	0.4	1.0	2.0	0.4
3	1.0	0.0	1000.0	1.0	0.0	0.01
4	1.0	0.0	0.01	1.0	0.0	100.0
5	5.99924	19.5975	460.894	5.99242	-6.19633	46.0950

Table 4.1. Data for five Riemann problem tests

Table 4.2 shows the computed values for pressure in the *Star Region* by solving the pressure equation $f(p) = 0$ (equation 4.5) by a Newton–Raphson method. This task is carried out by the subroutine RIEMANN, which is contained in the FORTRAN 77 program given in Sect. 4.9 of this chapter.

Test	p_*	p_{TR}	p_{PV}	p_{TS}	$\frac{1}{2}(p_L + p_R)$
1	0.30313	0.30677(3)	0.55000(5)	0.31527(3)	0.55(5)
2	0.00189	exact(1)	TOL(8)	TOL(8)	0.4(9)
3	460.894	912.449(5)	500.005(4)	464.108(3)	500.005(4)
4	46.0950	82.9831(5)	50.005(4)	46.4162(3)	50.005(4)
5	1691.64	2322.65(4)	781.353(5)	1241.21(4)	253.494(6)

Table 4.2 Guess values p_0 for iteration scheme. Next to each guess is the required number of iterations for convergence (in parentheses).

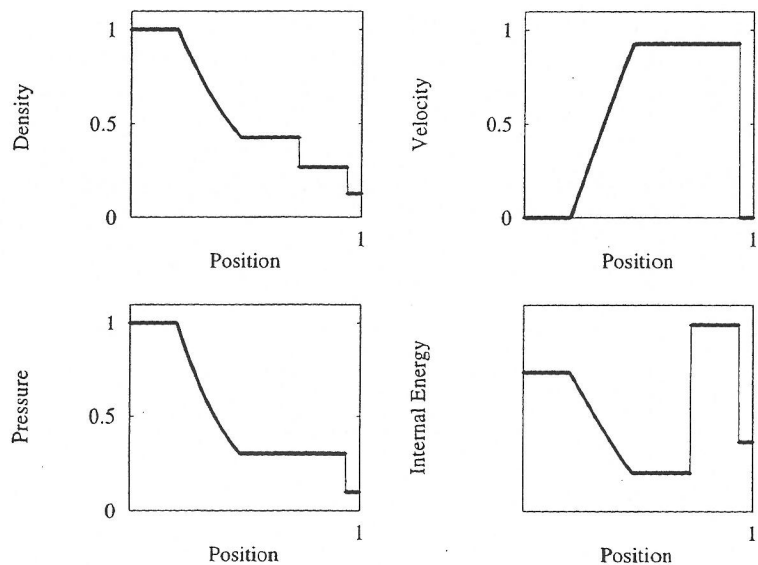


Fig. 4.7. Test 1: Exact solution for density, velocity, pressure and specific internal energy at time $t = 0.25$ units

The exact, converged, solution for pressure is given in column 2. Columns 3 to 6 give the guess values p_{TR} , p_{PV} , p_{TS} and the arithmetic mean value of the data. The number in parentheses next to each guess value is the number of iterations required for convergence for a tolerance $TOL = 10^{-6}$. For Test 1, p_{TR} and p_{TS} are the best guess values for p_0 . For Test 2, p_{TR} is actually the exact solution (two rarefactions). By excluding Test 2, p_{TS} is the best guess overall. Experience in using hybrid schemes suggests that a combination of two or three approximations is bound to provide a suitable guess value for p_0 that is both accurate and efficient. In the FORTRAN 77 program provided in Sect. 4.9 of this chapter, the subroutine STARTE contains a hybrid scheme

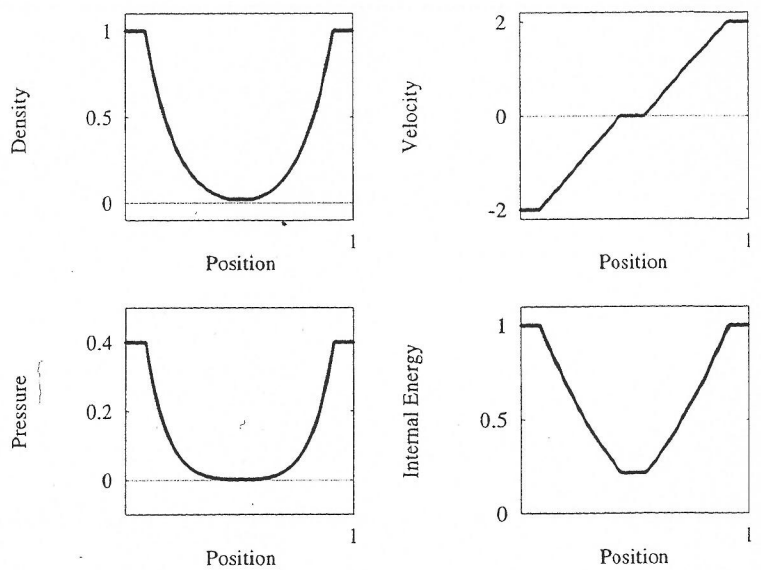


Fig. 4.8. Test 2: Exact solution for density, velocity, pressure and specific internal energy at time $t = 0.15$ units

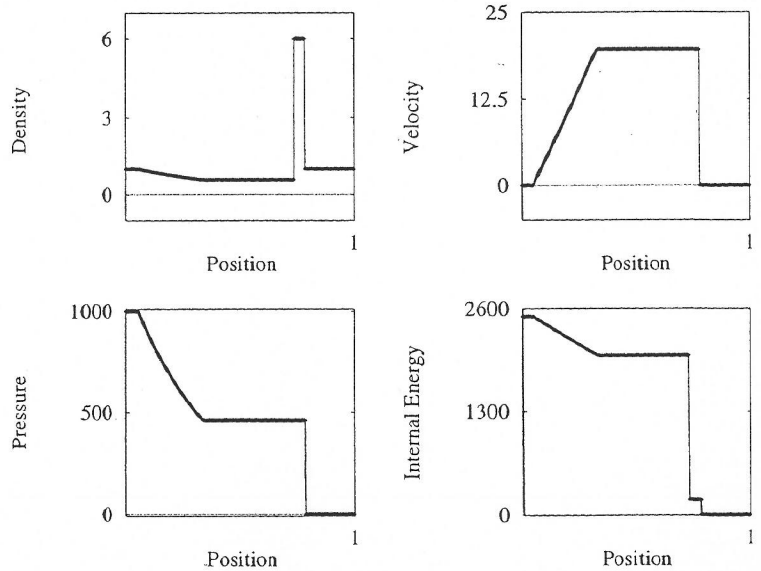


Fig. 4.9. Test 3: Exact solution for density, velocity, pressure and specific internal energy at time $t = 0.012$ units

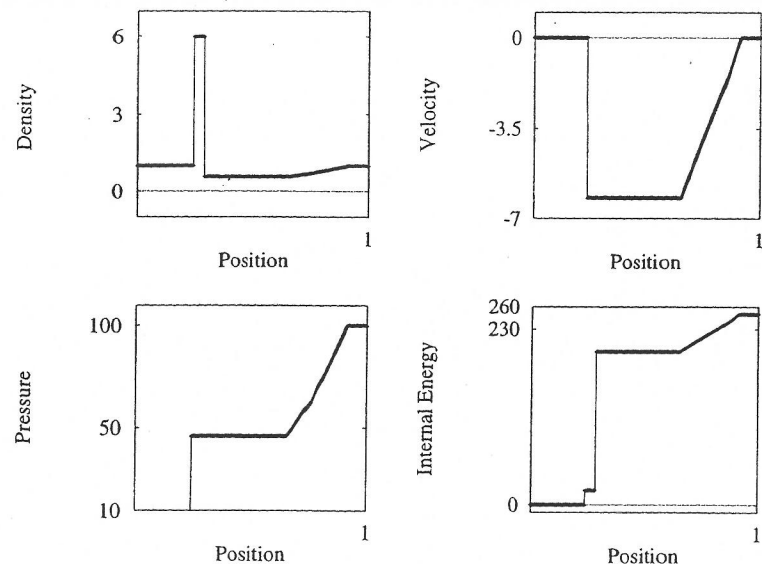


Fig. 4.10. Test 4: Exact solution for density, velocity, pressure and specific internal energy at time $t = 0.035$ units

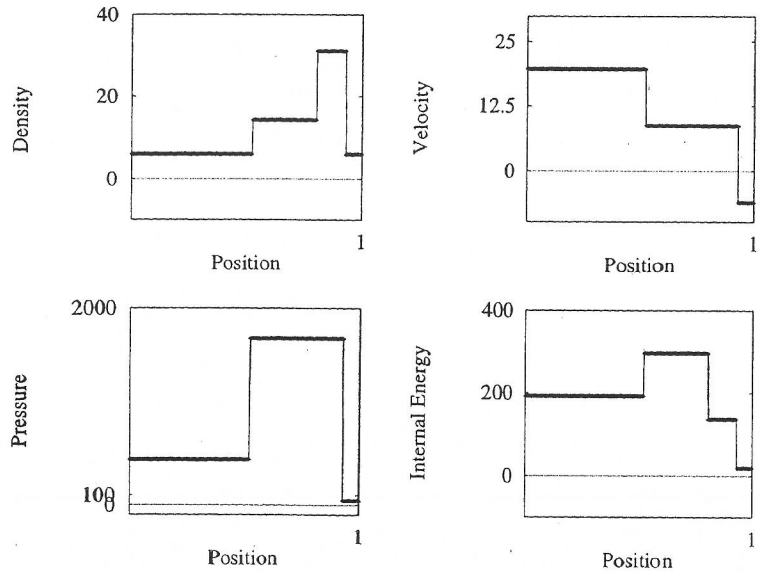


Fig. 4.11. Test 5: Exact solution for density, velocity, pressure and specific internal energy at time $t = 0.035$ units

involving p_{PV} , p_{TR} and p_{TS} . In a typical application of the exact Riemann solver to a numerical method, the overwhelming majority of Riemann problems will consist of *nearby states* which can be accurately approximated by the simple value p_{PV} .

Having found p_* , the solution u_* for the particle velocity follows from (4.9) and the density values ρ_{*L} , ρ_{*R} follow from appropriate wave relations, as detailed in the next section. Table 4.3 shows exact solutions for pressure p_* , speed u_* , densities ρ_{*L} and ρ_{*R} for tests 1 to 5. These quantities may prove of some use for initial testing of programs.

Test	p_*	u_*	ρ_{*L}	ρ_{*R}
1	0.30313	0.92745	0.42632	0.26557
2	0.00189	0.00000	0.02185	0.02185
3	460.894	19.5975	0.57506	5.99924
4	46.0950	-6.19633	5.99242	0.57511
5	1691.64	8.68975	14.2823	31.0426

Table 4.3. Exact solution for pressure, speed and densities for tests 1 to 5.

4.4 The Complete Solution

So far, we have an algorithm for computing the pressure p_* and particle velocity u_* in the *Star Region*. We still do not know the sought values ρ_{*L} and ρ_{*R} for the density in this region; these are computed by identifying the types of non-linear waves, which can be done by comparing the pressure p_* to the pressures p_L and p_R , and then applying the appropriate conditions across the respective waves. Another pending task is to determine completely the left and right waves. For shock waves we only need to find the density behind the wave and the shock speed. For rarefaction waves there is more work involved: we need ρ behind the wave, equations for the *Head* and *Tail* of the wave and the full solution inside the rarefaction fan.

There are two cases. First we consider the case in which the sampling point (x, t) lies to the left of the contact discontinuity, as in Fig. 4.12. Again, there are two possibilities; these are now studied separately.

Left Shock Wave. A left shock wave, see Fig. 4.12a, is identified by the condition $p_* > p_L$. We know p_* and u_* . From the pressure ratio, see Sect. 3.1.3 of Chap. 3, we find the density according to

$$\rho_{*L} = \rho_L \left[\frac{\frac{p_*}{p_L} + \frac{\gamma-1}{\gamma+1}}{\frac{\gamma-1}{\gamma+1} \frac{p_*}{p_L} + 1} \right]. \quad (4.50)$$

The shock speed S_L is also a function of the pressure p_* . From (4.10) and (4.14) we deduce the shock speed as

$$S_L = u_L - Q_L / \rho_L , \quad (4.51)$$

where the mass flux Q_L is given by (4.20). More explicitly, see Sect. 3.1.3 of Chap. 3, one has p. 102, (3.62); but much easier to obtain from (4.51)+(4.20) (since (3.62) follows from (3.6)) itself difficult to obtain from the analogous of (3.48)+(3.59)+(3.58))

$$S_L = u_L - a_L \left[\frac{\gamma+1}{2\gamma} \frac{p_*}{p_L} + \frac{\gamma-1}{2\gamma} \right]^{\frac{1}{2}} . \quad (4.52)$$

We have therefore completely determined the solution for the entire region to the left of the contact discontinuity in the case in which the left wave is a shock wave.

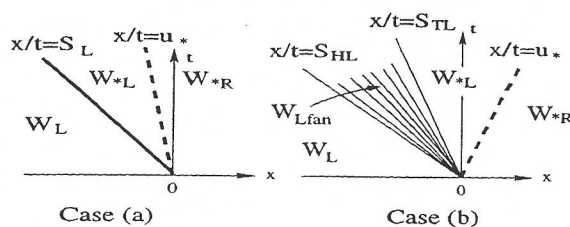


Fig. 4.12. Sampling the solution at a point to the left of the contact: (a) left wave is a shock (b) left wave is a rarefaction

Left Rarefaction Wave. A left rarefaction wave, see Fig. 4.12b, is identified by the condition $p_* \leq p_L$. The pressure p_* and the particle velocity u_* in the Star Region are known. The density follows from the isentropic law as

$$\rho_{*L} = \rho_L \left(\frac{p_*}{p_L} \right)^{\frac{1}{\gamma}} . \quad (4.53)$$

The sound speed behind the rarefaction is

$$a_{*L} = a_L \left(\frac{p_*}{p_L} \right)^{\frac{\gamma-1}{2\gamma}} . \quad (4.54)$$

The rarefaction wave is enclosed by the Head and the Tail, which are the characteristics of speeds given respectively by

$$S_{HL} = u_L - a_L , \quad S_{TL} = u_* - a_{*L} . \quad (4.55)$$

We now find the solution for $\mathbf{W}_{L\text{fan}} = (\rho, u, p)^T$ inside the left rarefaction fan. This is easily obtained by considering the characteristic ray through the origin $(0,0)$ and a general point (x,t) inside the fan. The slope of the characteristic is

$$\frac{dx}{dt} = \frac{x}{t} = u - a ,$$

where u and a are respectively the sought particle velocity and sound speed at (x,t) . Also, use of the Generalised Riemann Invariant $I_L(u, a)$ yields

$$u_L + \frac{2a_L}{\gamma-1} = u + \frac{2a}{\gamma-1} .$$

The simultaneous solution of these two equations for u and a , use of the definition of the sound speed a and the isentropic law give the result

$$\mathbf{W}_{L\text{fan}} = \begin{cases} \rho = \rho_L \left[\frac{2}{(\gamma+1)} + \frac{(\gamma-1)}{(\gamma+1)a_L} (u_L - \frac{x}{t}) \right]^{\frac{2}{\gamma-1}} , \\ u = \frac{2}{(\gamma+1)} \left[a_L + \frac{(\gamma-1)}{2} u_L + \frac{x}{t} \right] , \\ p = p_L \left[\frac{2}{(\gamma+1)} + \frac{(\gamma-1)}{(\gamma+1)a_L} (u_L - \frac{x}{t}) \right]^{\frac{2\gamma}{\gamma-1}} . \end{cases} \quad (4.56)$$

Next we consider the solution at a point (x,t) to the right of the contact discontinuity for the two possible wave configurations of Fig. 4.13.

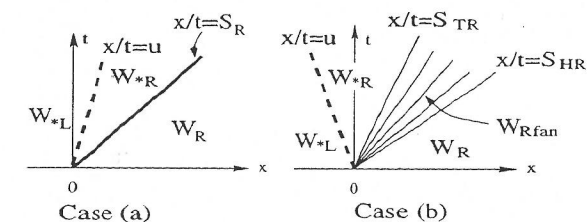


Fig. 4.13. Sampling the solution at a point to the right of the contact: (a) right wave is a shock (b) right wave is a rarefaction

Right Shock Wave. A right shock wave, see Fig. 4.13a, is identified by the condition $p_* > p_R$. We know the pressure p_* and the particle velocity u_* . The density ρ_{*R} is found to be

$$\rho_{*R} = \rho_R \left[\frac{\frac{p_*}{p_R} + \frac{\gamma-1}{\gamma+1}}{\frac{\gamma-1}{\gamma+1} \frac{p_*}{p_R} + 1} \right] \quad (4.57)$$

and the shock speed is

$$S_R = u_R + Q_R / \rho_R , \quad (4.58)$$

with the mass flux Q_R given by (4.30). More explicitly we have

$$S_R = u_R + a_R \left[\frac{(\gamma+1)}{2\gamma} \frac{p_*}{p_R} + \frac{(\gamma-1)}{2\gamma} \right]^{\frac{1}{2}} . \quad (4.59)$$

Right Rarefaction Wave. A right rarefaction wave, see Fig. 4.13b, is identified by the condition $p_* \leq p_R$. The pressure p_* and velocity u_* in the *Star Region* are known. The density is found from the isentropic law as

$$\rho_{*R} = \rho_R \left(\frac{p_*}{p_R} \right)^{\frac{1}{\gamma}}, \quad (4.60)$$

from which the sound speed follows as

$$a_{*R} = a_R \left(\frac{p_*}{p_R} \right)^{\frac{\gamma-1}{2\gamma}}. \quad (4.61)$$

The speeds for the *Head* and *Tail* are given respectively by

$$S_{HR} = u_R + a_R, \quad S_{TR} = u_* + a_{*R}. \quad (4.62)$$

The solution for $\mathbf{W}_{R\text{fan}}$ inside a right rarefaction fan is found in an analogous manner to the case of a left rarefaction fan. The solution is

$$\mathbf{W}_{R\text{fan}} = \begin{cases} \rho = \rho_R \left[\frac{2}{(\gamma+1)} - \frac{(\gamma-1)}{(\gamma+1)a_R} (u_R - \frac{x}{t}) \right]^{\frac{2}{\gamma-1}}, \\ u = \frac{2}{(\gamma+1)} \left[-a_R + \frac{(\gamma-1)}{2} u_R + \frac{x}{t} \right], \\ p = p_R \left[\frac{2}{(\gamma+1)} - \frac{(\gamma-1)}{(\gamma+1)a_R} (u_R - \frac{x}{t}) \right]^{\frac{2\gamma}{\gamma-1}}. \end{cases} \quad (4.63)$$

4.5 Sampling the Solution

We have developed a solver to find the exact solution of the complete wave structure of the Riemann problem at any point (x, t) in the relevant domain of interest $x_L < x < x_R$; $t > 0$, with $x_L < 0$ and $x_R > 0$. We now provide a solution sampling procedure which, apart from being a summary of the solution, may also prove of practical use when programming the solution algorithm. Suppose we wish to evaluate the solution at a general point (x, t) . We denote the solution of the Riemann problem at (x, t) in terms of the vector of primitive variables $\mathbf{W} = (\rho, u, p)^T$. As the solution \mathbf{W} is a similarity solution we perform the sampling in terms of the *speed* $S = x/t$. When the solution at a specified time t is required the solution profiles are only a function of space x . In sampling the complete solution there are two cases to consider.

4.5.1 Left Side of Contact: $S = x/t \leq u_*$

As shown in Fig. 4.12 there are two possible wave configurations. Fig. 4.12a shows the case in which the left wave is a shock wave. In this case the complete solution on the left hand side of the contact wave is

$$\mathbf{W}(x, t) = \begin{cases} \mathbf{W}_{*L}^{\text{sho}} \text{ if } S_L \leq \frac{x}{t} \leq u_*, \\ \mathbf{W}_L \text{ if } \frac{x}{t} \leq S_L, \end{cases} \quad (4.64)$$

where S_L is the shock speed given by (4.52), $\mathbf{W}_{*L}^{\text{sho}} = (\rho_{*L}^{\text{sho}}, u_*, p_*)^T$ with ρ_{*L}^{sho} given by (4.50) and \mathbf{W}_L is the left data state. If the left wave is a rarefaction, as depicted by Fig. 4.12b, then the complete solution on the left hand side of the contact consists of three states, namely

$$\mathbf{W}(x, t) = \begin{cases} \mathbf{W}_L & \text{if } \frac{x}{t} \leq S_{HL}, \\ \mathbf{W}_{L\text{fan}} & \text{if } S_{HL} \leq \frac{x}{t} \leq S_{TL}, \\ \mathbf{W}_{*L}^{\text{fan}} & \text{if } S_{TL} \leq \frac{x}{t} \leq u_*, \end{cases} \quad (4.65)$$

where S_{HL} and S_{TL} are the speeds of the head and tail of the rarefaction given by (4.55), $\mathbf{W}_{*L}^{\text{fan}} = (\rho_{*L}^{\text{fan}}, u_*, p_*)^T$ with ρ_{*L}^{fan} given by (4.53), $\mathbf{W}_{L\text{fan}}$ is the state inside the rarefaction fan given by (4.56) and \mathbf{W}_L is the left data state. Fig. 4.14 shows a flow chart for sampling the solution at any point (x, t) to the left of the contact discontinuity.

4.5.2 Right Side of Contact: $S = x/t \geq u_*$

As shown in Fig. 4.13 there are two possible wave configurations. Fig. 4.13a shows the case in which the right wave is a shock wave. In this case the complete solution on the right hand side of the contact wave is

$$\mathbf{W}(x, t) = \begin{cases} \mathbf{W}_{*R}^{\text{sho}} & \text{if } u_* \leq \frac{x}{t} \leq S_R, \\ \mathbf{W}_R & \text{if } \frac{x}{t} \geq S_R, \end{cases} \quad (4.66)$$

where S_R is the shock speed given by (4.59), $\mathbf{W}_{*R}^{\text{sho}} = (\rho_{*R}^{\text{sho}}, u_*, p_*)^T$ with ρ_{*R}^{sho} given by (4.57) and \mathbf{W}_R is the right data state. If the right wave is a rarefaction, as depicted by Fig. 4.13b, then the complete solution on the right hand side of the contact consists of three states, namely

$$\mathbf{W}(x, t) = \begin{cases} \mathbf{W}_{*R}^{\text{fan}} & \text{if } u_* \leq \frac{x}{t} \leq S_{TR}, \\ \mathbf{W}_{R\text{fan}} & \text{if } S_{TR} \leq \frac{x}{t} \leq S_{HR}, \\ \mathbf{W}_R & \text{if } \frac{x}{t} \geq S_{HR}, \end{cases} \quad (4.67)$$

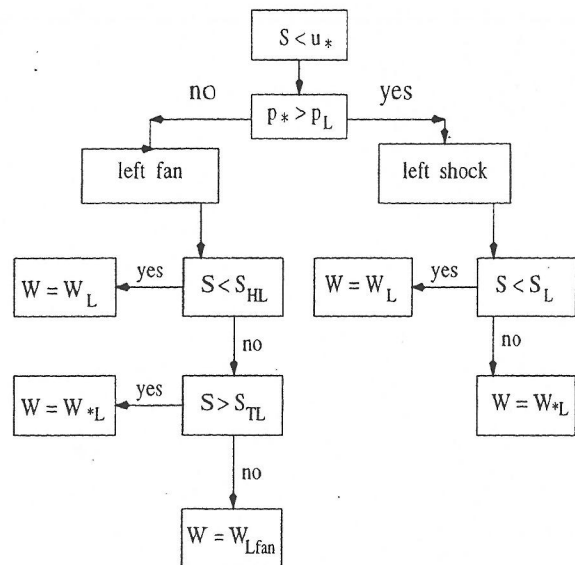


Fig. 4.14. Flow chart for sampling the solution at a point (x, t) to the left of the contact discontinuity $\frac{dx}{dt} = u_*$; $S = x/t$

where S_{HR} and S_{TR} are the speeds of the head and tail of the rarefaction given by (4.62), $\mathbf{W}_{*R}^{\text{fan}} = (\rho_{*R}^{\text{fan}}, u_{*R}^{\text{fan}}, p_{*R}^{\text{fan}})^T$ with ρ_{*R}^{fan} given by (4.60), $\mathbf{W}_{R\text{fan}}$ is the state inside the right rarefaction fan given by (4.63) and \mathbf{W}_R is the right data state.

Exercise 4.5.1. Write a flow chart for sampling the solution at any point (x, t) to the right of the contact discontinuity $\frac{dx}{dt} = u_*$.

Solution 4.5.1. (Left to the reader).

4.6 The Riemann Problem in the Presence of Vacuum

The admission of flowing material adjacent to *vacuum* plays an important role in a number of practical applications. Loosely, vacuum is characterised by the condition $\rho = 0$. It follows that the total energy per unit mass also vanishes, $E = 0$. Values of pressure and particle velocity in vacuum are discussed later. Naturally, in vacuum regions the Euler equations, or any other mathematical model based on the continuum assumption, are no longer a valid description of the Physics. As for the non-vacuum case described previously, the simplest problem involving the vacuum state is furnished by the Riemann problem. There are two obvious cases to consider. One is that in which the left non-vacuum state is adjacent to a right vacuum state at the initial time $t = 0$. The

second case is simply the previous case reversed, the right non-vacuum state is adjacent to a left vacuum state. There is a third case, in which both left and right data states are non-vacuum states, but the vacuum state is generated in the interaction of the data states via the Riemann problem. The solution of the Riemann problem in the presence of vacuum involves the computation of free boundaries separating vacuum regions from those in which material exists.

In the presence of vacuum the structure of the solution of the Riemann problem is different from that of the conventional case shown in Fig. 4.1. The *Star Region* does not exist. Attempts at using the pressure equation (4.5) and an iterative scheme to solve it will fail, simply because the scheme would be assuming a solution structure that does not exist. The temptation to use *small values* of density and pressure to *simulate* vacuum with the Riemann solver for the non-vacuum case will also prove frustrating. If this is done in approximate Riemann solvers, then one is effectively changing the local wave structure of the solution.

Concerning the admissible elementary waves present in the structure of the solution of the Riemann problem including the vacuum state, an important observation is that a shock wave cannot be adjacent to a vacuum region. This is stated in the following proposition

Proposition 4.6.1. *A shock wave cannot be adjacent to a vacuum region.*

Proof. Let us consider a left non-vacuum constant state $\mathbf{W}_L = (\rho_L, u_L, p_L)^T$ adjacent to a right vacuum state $\mathbf{W}_0 \equiv (\rho_0, u_0, p_0)^T$ at the initial time $t = 0$, where $\rho_0 = 0$. Assume these states are connected by a discontinuity of speed S . Application of the Rankine–Hugoniot Conditions, see Sect. 3.1.3 of Chap. 3, gives

$$\rho_L u_L - \rho_0 u_0 = S(\rho_L - \rho_0), \quad (4.68)$$

$$\rho_L u_L^2 + p_L - (\rho_0 u_0^2 + p_0) = S(\rho_L u_L - \rho_0 u_0), \quad (4.69)$$

$$u_L(E_L + p_L) - u_0(E_0 + p_0) = S(E_L - E_0). \quad (4.70)$$

As $E_0 = 0$ and assuming u_0 to be *finite*, manipulation of the equations gives

$$u_L = u_0 = S, \quad p_L = p_0. \quad (4.71)$$

It follows that a shock wave cannot be adjacent to a region of vacuum, $p_L = p_0$. The proposition is thus proved.

From the result (4.71) it also follows that a contact discontinuity can be adjacent to a region of vacuum, $u_L = u_0 = S$, which makes perfect physical sense. This wave separates a region of material from a region of no material and is therefore a boundary. The velocity u_0 of the front is also the maximum particle velocity across the wave system connecting a non-vacuum state with the vacuum state and is called the *escape velocity*. It turns out that u_0 is